

Article

Nitrogen Oxides and Ammonia Removal Analysis Based on Three-Dimensional Ammonia-Diesel Dual Fuel Engine Coupled with One-Dimensional SCR Model

Xingyu Sun ¹, Mengjia Li ^{2,*}, Jincheng Li ^{2,*}, Xiongbo Duan ³, Can Wang ², Weifan Luo ², Haifeng Liu ^{2,*}  and Jingping Liu ¹

¹ College of Mechanical and Vehicle Engineering, Hunan University, Changsha 410082, China

² State Key Laboratory of Engines, Tianjin University, Tianjin 300072, China

³ School of Energy Science and Engineering, Central South University, Changsha 410083, China

* Correspondence: lmjqaq3721@163.com (M.L.); 1019201082@tju.edu.cn (J.L.); haifengliu@tju.edu.cn (H.L.)

Abstract: Ammonia, as an alternative fuel for internal combustion engines, can achieve nearly zero carbon emissions. Although the development of the pure ammonia engine is limited by its poor combustion characteristics, ammonia–hydrocarbon mixed combustion can effectively improve the combustion of ammonia fuel. With the increase in the ammonia fuel proportion in the fuel mixture, a large number of nitrogen oxides (NO_x) and unburned ammonia may be discharged, which have a poor impact on the environment. In this study, the performance of selective catalytic reduction (SCR) aftertreatment technology in reducing NO_x and ammonia emissions from ammonia–diesel dual-fuel engines was investigated using simulation. A good cross-dimensional model was established under the coupling effect, though the effect of a single-dimensional model could not be presented. The results show that when the exhaust gas in the engine cylinder is directly introduced into the SCR without additional reducing agents such as urea, unburned ammonia flowing into SCR model is in excess, and there will be only ammonia at the outlet; however, if the unburned ammonia fed into the SCR model is insufficient to reduce NO, the ammonia concentration at the outlet will be 0. NO_x can be 100% effectively reduced to N₂ under most engine conditions; thus, unburned ammonia in exhaust plays a role in reducing NO_x emissions from ammonia–diesel dual-fuel engines. However, when the concentration of unburned ammonia in the exhaust gas of an ammonia–diesel dual-fuel engine is large, its ammonia emissions are still high even after the SCR. In addition, the concentrations of N₂O after SCR do not decrease, but increase by 50.64 in some conditions, the main reason for which is that by the action of the SCR catalyst, NO₂ is partially converted into N₂O, resulting in an increase in its concentration at the SCR outlet. Adding excessive air or oxygen into the SCR aftertreatment model can not only significantly reduce the ammonia concentration at the outlet of the model without affecting the NO_x conversion efficiency of SCR, but inhibit N₂O production to some extent at the outlet, thus reducing the unburned ammonia and NO_x emissions in the tail gas of ammonia–diesel dual-fuel engines at the same time without the urea injection. Therefore, this study can provide theoretical guidance for the design of ammonia and its mixed-fuel engine aftertreatment device, and provide technical support for reducing NO_x emissions of ammonia and its mixed fuel engines.

Keywords: ammonia–diesel dual-fuel engines; nitrogen oxides emissions; selective catalytic reduction (SCR); without the urea



Citation: Sun, X.; Li, M.; Li, J.; Duan, X.; Wang, C.; Luo, W.; Liu, H.; Liu, J. Nitrogen Oxides and Ammonia Removal Analysis Based on Three-Dimensional Ammonia-Diesel Dual Fuel Engine Coupled with One-Dimensional SCR Model. *Energies* **2023**, *16*, 908. <https://doi.org/10.3390/en16020908>

Academic Editor: Dimitrios C. Rakopoulos

Received: 13 December 2022

Revised: 9 January 2023

Accepted: 10 January 2023

Published: 13 January 2023



Copyright: © 2023 by the authors. Licensee MDPI, Basel, Switzerland. This article is an open access article distributed under the terms and conditions of the Creative Commons Attribution (CC BY) license (<https://creativecommons.org/licenses/by/4.0/>).

1. Introduction

Continually increasing greenhouse emissions caused by human activities have led to terrible climate change. Millions of people and many natural systems suffer from climate-related hazards [1]. So, reducing emissions of greenhouse gases such as CO₂ is an urgent need to slow global warming [2], and reducing the use of hydrocarbon fuels is key to reducing emissions. In this scenario, ammonia has been considered as an alternative fuel to

combustion devices [3,4], particularly in the internal combustion engine [5–10]. The carbon reduction measures in internal combustion engines mainly include advanced in-cylinder combustion technology, hybrid power systems, and net-zero carbon fuel combustion technology, all of which have promoted the development of ammonia as an ideal alternative fuel for internal combustion engines that emit no carbon dioxide [11]. First of all, ammonia is a carbon-free fuel; no carbon dioxide is produced during its combustion so the carbon emission problem would be solved. It is also possible to use renewable energy to produce ammonia [12,13]. All cycles produce no carbon emissions in their “preparation-use” processes [14–16]. In addition, as shown in Table 1, compared to other standard fuels, ammonia is easy to liquify, while the storage, transportation, and distribution of liquid ammonia are relatively more accessible and safer compared to hydrogen, and it has high energy density per unit volume, as well as a high octane number, which is conducive to the popularization of internal combustion engines. Another advantage of ammonia as fuel is that the procedures for safe handling of large quantities are well established and documented and the infrastructure for its transportation by rail, road or pipelines exists in many countries. The interest in deploying ammonia as a potential low-carbon fuel is increasing, and it is projected that the ammonia market will grow up to 3% in the upcoming ten years, while it will be labelled as one of the new conventional fuel sources [17]. However, as shown in Table 2 and combined with Table 1, the low laminar flame velocity, low calorific value, high self-ignition temperature, and high ignition energy in the combustion process of pure ammonia fuel limit its development as a single fuel for internal combustion engines [18,19].

Table 1. Comparison of main physical and chemical properties of ammonia with hydrogen, natural gas, gasoline and diesel.

| Properties | Ammonia | Hydrogen | Hydrogen | Natural Gas | Gasoline | Diesel |
|--|-------------------|-------------------|----------------|-------------------|----------|---------|
| Storage method | compressed liquid | compressed liquid | compressed gas | compressed liquid | liquid | liquid |
| Storage temperature (K) | 298 | 20 | 298 | 298 | 298 | 298 |
| Storage pressure (kPa) | 1030 | 102 | 24,821 | 24,821 | 101.3 | 101.3 |
| Autoignition temperature (K) | 924 | 844 | 844 | 723 | 573 | 503 |
| Flammability limits (Vol. %) | 16–25 | 4–75 | 4–75 | 5–15 | 1.4–7.6 | 0.6–7.5 |
| Absolute minimum (MJ) | 8 | - | 0.02 | - | 0.14 | - |
| Fuel density @20 °C (kg/m ³) | 602.8 | 71.1 | 17.5 | 187.2 | 698.3 | 838.8 |
| Energy density (MJ/m ³) | 11,333 | 8539 | 2101 | 7132 | 31,074 | 36,403 |
| Octane rating (RON) | 130 | >130 | >130 | 107 | 90–98 | - |

Table 2. Physicochemical characteristics of fuel-air mixture.

| | Ammonia | Gasoline | Natural Gas | Hydrogen | Methanol |
|---|---------|----------|-------------|----------|----------|
| Lower heating value (MJ/kg) | 18.8 | 44.5 | 50 | 120 | 19.9 |
| Theoretical air/fuel ratio | 6.06 | 14.5 | 17.16 | 34.5 | 6.43 |
| Equivalent mole fraction | 0.22 | 0.02 | 0.095 | 0.00296 | 0.12 |
| Equivalent mole mass calorific value (kJ/mol) | 70.31 | 95.23 | 76 | 71.01 | 76.42 |
| Laminar flame velocity@20 °C & 1 atm (cm/s) | 7 | 43 | 38 | 351 | 36 |

Based on the above problems and exploration, many studies have shown that the mixed combustion of ammonia and other promoters can solve the problems about the combustion characteristics of pure ammonia combustion, and when a small percentage of other fuels are added as combustion promoters, ammonia can be effectively used as fuel for internal combustion engines. Among them, hydrogen is certainly the most valuable since it is carbon-free and has opposed and complementary characteristics to those of

ammonia [20,21]. Wang et al. [22] showed that most properties of ammonia-hydrogen combustion could be comparable to that of hydrocarbon fuels under engine-relevant conditions, and the studies have shown that ammonia and hydrogen mixtures have better performance and knock resistance at higher compression ratios and are more suitable for working at higher compression ratios. Li et al. [23] and Frigo et al. [24] found that increases in ammonia injection pressure and H₂ ratio can significantly reduce the ignition delay time of NH₃ mixtures and promote the ignition of NH₃ [23,24]. However, the NO_x emission concentration of the mixed combustion of ammonia and hydrogen at full load has reached 1500–1700 ppm, which is unlikely to meet the current emission regulations even with an aftertreatment [9].

In addition to hydrogen as a combustion promoter, there are also studies on the combustion experiments of ammonia and the dual-fuel hybrid combustion of other fuels such as diesel, gasoline or dimethyl ether. Relevant studies showed that with different proportions of ammonia and gasoline fuel mixed-combustion tests, using ammonia in a certain operating range presented better engine performance than gasoline alone, and ammonia could be used instead of gasoline in a limited working range, but its NO_x emissions increased significantly with the increase in ammonia concentrations [14,16,25,26]. Similarly, combustion experiments on diesel engines with different ammonia and diesel mixture ratios showed that the fuel consumption of the engine improved, but NO_x emissions increased accordingly [27,28]. Ryu et al. [29] and Gross et al. [30] conducted an engine experiment about the mixed combustion of dimethyl ether and ammonia, and found that the in-cylinder combustion pressure and temperature were low and the combustion in the cylinder was not sufficient, resulting in the deterioration of engine emission performance.

The above-mentioned experimental studies on ammonia and its blends show that the engine's fuel consumption improved. The engine significantly reduces carbon emissions such as CO₂ with the reduction of the hydrocarbon combustion promoter, but the NO_x emissions dramatically increase. The main reason for the high NO_x emissions from the combustion of ammonia fuel and its blends engines is the high nitrogen content of ammonia. The NO_x emissions can cause a variety of impacts on the environment and the human body, so the elimination of NO_x and other pollutants has become the hottest issue in the field of air pollution control [31,32].

Under this topic, engine technologies for reducing NO_x emissions from ammonia and its blends can be divided into two categories: advanced in-cylinder combustion control technology and exhaust gas control technology. Advanced in-cylinder combustion control technologies mainly include fuel injection control technology, advanced combustion technology, and exhaust gas recirculation (EGR) technology [33]. Since the research on ammonia and its blends engines is still in its infancy, even combined with the traditional internal combustion engine emission reduction research status, to meet NO_x emissions standard from ammonia and its blends simply using advanced in-cylinder combustion control technology engines is almost impossible. In addition, the simulation and comparison of engine emissions in the current literature are mostly the analysis of single-dimensional results. For example, it is mentioned in the literature that a three-dimensional ammonia engine model is established to evaluate the performance and emission characteristics of the ammonia engine, including the NO_x and CO₂ emission levels of the engine and the unburned ammonia gas. Although the NO_x emission of this operation mode can reach the limit of Tier II emission, most of them do not consider the level change in N₂O emissions [34,35]. In recent years, the application of SCR technology in NO_x exhaust control has been favored by the automotive industry, not only because of its high conversion rate, good selectivity, strong practicality and other characteristics, but also because of the lower cost of SCR technology compared with other systems [36]. Moreover, related studies show that SCR aftertreatment technology is a powerful means to greatly reduce nitrogen oxide emissions from ammonia and its mixed fuel engines [37,38]. However, in the validation of SCR models and in the emission literature, most studies are one-dimensional simulations of the possibility of using residual ammonia in the ammonia–diesel dual fuel to activate

selective catalytic reduction (SCR) systems, indicating that residual ammonia from the dual fuel compression engine can be successfully run into the aftertreatment SCR model. However, the author did not establish the relationship between the three-dimensional engine model and the one-dimensional SCR aftertreatment model [39,40].

In short, SCR aftertreatment technology is crucial in reducing ammonia engine emissions, and increasingly stringent emission regulations drive its hybrid fuel engines forward [41–43]. However, single-dimensional simulation results alone cannot realize the relationship between a one-dimensional model and a three-dimensional model and their respective algorithm advantages. Therefore, the author first coupled a set of simplified chemical reaction kinetics mechanisms for ammonia–diesel dual-fuel to a 3D CONVERGE ammonia–diesel dual-fuel engine and verified its in-cylinder combustion with the help of engine test data. Then, the one-dimensional SCR post-processing model verified by the test was coupled with the engine model. The author analyzed the efficiency of SCR in reducing the NO_x emission of the engine under different operating conditions of ammonia and its mixed-fuel engine. The strategy is presented here of “adding excessive air” for SCR to achieve removal of ammonia NO_x and inhibit N₂O production at the same time under certain engine operating conditions without the urea. The design of the aftertreatment device provides theoretical guidance and technical support for reducing the NO_x emission of ammonia and its mixed-fuel engine. The difference from the traditional SCR aftertreatment device is that the incompletely combusted ammonia in the engine is directly fed into the SCR model to explore the emission reduction efficiency of the model under different engine operating conditions; however, the traditional SCR only relies on the spray reduction of urea aqueous solution.

2. Model Validation and Research Method

2.1. The Engine Model and Its Validation

The engine model of Niki et al. [44] is the basis for the establishment of the 3D CONVERGE engine model in this study, which is a naturally aspirated single-cylinder diesel engine. Its structure and operating parameters are shown in Table 3, among which 0 °CA is defined as the crankshaft rotation angle corresponding to the top dead center.

Table 3. Engine structure and operating parameters.

| Parameters | Value |
|----------------------------------|-----------|
| Bore × stroke (mm) | 112 × 110 |
| Rated speed (rpm) | 1500 |
| Diesel injection time (°CA ATDC) | −8 |
| Diesel injection quantity (mg) | 27.2 |
| Ammonia flow rate (L/min) | 13.3 |

Based on the 3D simulation software CONVERGE, the calculation grid of the ammonia–diesel dual-fuel engine is established, including the combustion chamber and the fuel injection valve, as shown in Figure 1. It should be noted that the diesel fuel is introduced by high-pressure direct injection into the cylinder and ammonia is injected into the inlet. The parameters of the diesel injector are shown in Table 4. The model adopts the simplified mechanism of ammonia/n-heptane dual fuel with 13.3.



Figure 1. Schematic diagram of 3D model of ammonia-diesel dual-fuel engine.

Table 4. Parameters of diesel injection.

| Parameters | Value |
|-----------------------------------|--------------|
| Numbers of injector \times hole | 1×4 |
| Nozzle diameter (mm) | 0.31 |
| Spray duration ($^{\circ}$ CA) | 8.903 |
| Injection pressure (MPa) | 18 |

To consider the calculation accuracy and efficiency, after analyzing the grid sensitivity, the actual grid size is set to 2 cm, the minimum grid size for local refinement is 5 mm, and an adaptive mesh refinement (AMR) based on velocity and temperature is added. The maximum number of calculation grids is about 1.2 million, which can realize efficient and high-precision calculation. Figure 2 shows the comparison of cylinder pressure and heat release rate calculated by experiment and simulation; the experimental data are from the study of Niki et al. [44]. The red dotted line represents the cylinder pressure and heat release rate in the three-dimensional simulation, while the black solid line represents the cylinder pressure and heat release rate in the experimental results. The cylinder pressure was measured by a pressure transducer with a charge amplifier (Kistler 601 A and Type 5011). The cylinder pressure was measured every 1 crank angle degree and averaged 50 engine cycles. The gas analyzer measures multi-gas components at the same time. This analyzer can sample the hot exhaust gas. Its sampling line and sampling filter are heated to 191 $^{\circ}$ C. Thus, the NH_3 in exhaust gas containing H_2O can be detected precisely. The maximum burst pressure of the experiment is 6.2 MPa, the simulated value is 6.03 MPa, and the error is 2.7%; The crankshaft rotation angle corresponding to the experiment CA50 is 12.6 $^{\circ}$ CA, the simulation value is 10.05 $^{\circ}$ CA, and the error is 2.55 $^{\circ}$ CA. Under this condition, the experimental NO emission is 662 ppm, the NO emission predicted by the model is 573.6 ppm, and the error is 13.3%. Because the model can only reflect the results of the experiment to a large extent, it cannot fully present the results of the experiment, which is inevitable. The article cited that the prediction error of pollutants in the calibration content of the aftertreatment model had exceeded 10%. Generally, the prediction range of gas concentration within 15% is reasonable. Moreover, the cylinder pressure and heat release rate calculated by the simulation are in good agreement with the experimental results. That is, the model can accurately predict the actual working process of the engine and the emission of nitrogen oxides.

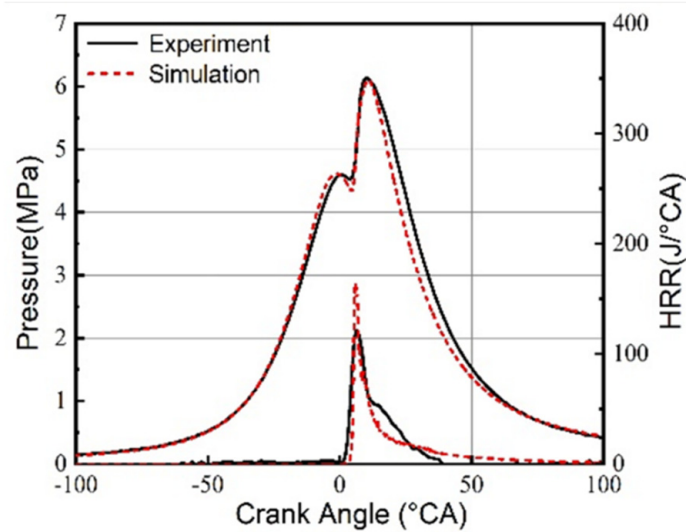


Figure 2. Comparison between simulation and experiment results of combustion pressure and heat release rate in cylinder.

2.2. The SCR Model and Its Validation

In addition to the research focus on ammonia–diesel dual-fuel engines and high NO_x emissions, the emission of unburned NH₃ is also a big challenge due to the toxic and corrosive properties of ammonia. In order to explore the reduction effect of the remaining NH₃ on NO_x in the cylinder under the coupling of SCR aftertreatment technology, the SCR aftertreatment model built by Li et al. [45] was coupled to the above ammonia–diesel dual-fuel engine. The evolution of NO_x without adding ammonia to the SCR system was analyzed. GT-power is used to establish the SCR quick-reaction kinetic model based on the reaction mechanism of Pant’s Cu-based zeolite [46]. The model is based on the following assumptions. (1) When calibrating the SCR model, to simplify the model processing, gaseous NH₃ is directly injected into the reactor without considering the spray and hydrolysis process of urea solution. The SCR reaction is described by the E-R mechanism [47], which considers that the response occurs between adsorbed NH₃ and NO_x in gas phase or weakly adsorbed state. The physical model of the SCR is shown in Figure 3. The model parameters are shown in Table 5, and the size of the model is modified based on the parameters mentioned earlier of the ammonia–diesel dual-fuel engine.

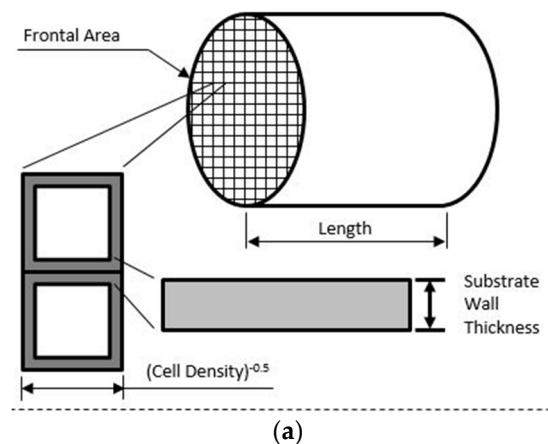


Figure 3. Cont.

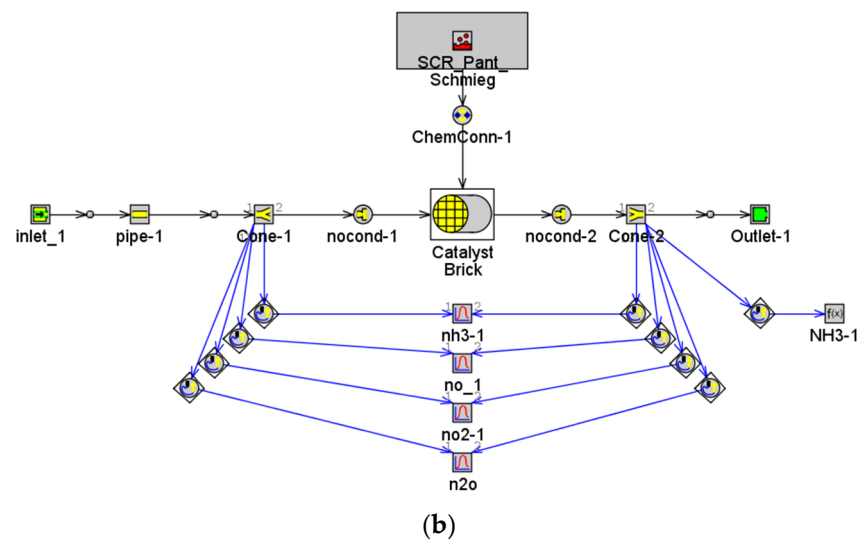


Figure 3. Schematic diagram of SCR model. (a) SCR physical model. (b) SCR one-dimensional model.

Table 5. Parameters of SCR mode.

| Parameters | Value |
|---|---------|
| Cross sectional area (cm ²) | 558.386 |
| Length (cm) | 2.464 |
| Cell density (cps) | 400 |
| Wall thickness (cm) | 0.010 |

As shown in Figure 4, according to the ER mechanism, the primary reaction process of NH₃ selective catalytic reduction of NO is as follows:

- (1) NH₃ is adsorbed on the active site of the catalyst through external and internal diffusion;
- (2) NO diffuses externally and internally to the adsorbed NH₃ surface;
- (3) Catalytic reaction between gaseous NO and adsorbed NH₃ to generate N₂ and H₂O.

Table 6 shows the main reactions in the SCR catalytic converter. As shown in Reactions 1 and 2, NH₃(g) in the exhaust pipe is first adsorbed to the empty active site θ_{free} of the catalyst and becomes adsorbed NH₃*. Adsorption occurs when the adsorption rate is higher than the desorption rate.

Table 6. Main reactions and expressions in SCR catalytic converters.

| Reactions | Reaction Expressions | Pre-Exponent Multiplier | Activation Energy J/mol | No. |
|----------------------------|---|-------------------------|-------------------------|-----|
| Adsorption | $\text{NH}_3(\text{g}) + \theta_{\text{free}} \rightarrow \text{NH}_3^*$ | 4.5 | 0 | 1 |
| Desorption | $\text{NH}_3^* \rightarrow \text{NH}_3(\text{g}) + \theta_{\text{free}}$ | 2.49×10^5 | 0 | 2 |
| NH ₃ Oxidation | $4\text{NH}_3 + 5\text{O}_2 \rightarrow 4\text{NO} + 6\text{H}_2\text{O}$ | 1.39×10^6 | 63,800 | 3 |
| Standard SCR | $4\text{NH}_3^* + 4\text{NO} + \text{O}_2 \rightarrow 4\text{N}_2 + 6\text{H}_2\text{O} + 4\theta_{\text{free}}$ | 3.18×10^8 | 88,000 | 4 |
| Fast SCR | $2\text{NH}_3^* + \text{NO} + \text{NO}_2 \rightarrow 2\text{N}_2 + 3\text{H}_2\text{O} + 2\theta_{\text{free}}$ | 2.33×10^7 | 32,100 | 5 |
| Slow SCR | $4\text{NH}_3^* + 3\text{NO}_2 \rightarrow 3.5\text{N}_2 + 6\text{H}_2\text{O} + 4\theta_{\text{free}}$ | 4.24×10^5 | 58,300 | 6 |
| Formation N ₂ O | $2\text{NH}_3^* + 2\text{NO}_2 \rightarrow \text{N}_2 + \text{N}_2\text{O} + 3\text{H}_2\text{O} + 2\theta_{\text{free}}$ | 3.07×10^4 | 48,200 | 7 |
| NO Oxidation | $\text{NO} + 0.5\text{O}_2 \rightarrow \text{NO}_2$ | 3.63 | 32,100 | 8 |

Reactions 4, 5 and 6 only occur between NO_x in the exhaust pipe and NH₃* in the adsorbed state. The specific reactions involved in the reaction process are related to the ratio of NO₂ to NO_x. When the ratio of NO₂ to NO_x is 1, only Reaction 6 occurs; the ratio is between 1 and 0.5, reaction 5 occurs first, while the remaining NO₂ reacts as per 6. If the

ratio is 0.5, Reaction 5 occurs. When the ratio is between 0.5 and 0, Reaction 5 occurs first and the remaining NO participates in Reaction 4. If there is no NO₂ in the exhaust pipe, that is, the ratio is zero, NO participates in Reaction 4. Reaction 7 represents the formation of N₂O. Reaction 8 represents the oxidation of NO to NO₂.

When the concentration of NO_x in the exhaust is too low or the concentration of gaseous NH₃(g) is too high, the consumption rate of adsorbed NH₃* in SCR is slow, and the accumulated adsorbed NH₃* will exceed the maximum ammonia storage capacity of SCR, so that the SCR no longer has the required ammonia adsorption capacity, resulting in the direct emission of gaseous NH₃(g). In addition, adsorption NH₃* oxidation side Reaction 3 occurs in the SCR at high temperatures (>400 °C). If there is no SCR catalytic converter, then the above reactions will not occur, and gaseous NH₃ and NO_x in the exhaust pipe will be directly discharged into the atmosphere, causing environmental pollution.

It can be seen that the NH₃ adsorption and desorption reaction is an essential part of the standard SCR reaction. Therefore, the validation of ammonia adsorption and desorption is crucial. Figure 5 shows the comparison between the simulation results of the NH₃ adsorption and desorption model and the experimental results; data were obtained from the experimental test, and catalyst sample test data is provided by catalyst supplier. As shown in Figure 5, it can be seen that no matter the process of isothermal adsorption, isothermal desorption, or desorption at elevated temperature by which the reaction occurs, the errors between the simulation results and the experimental data are all within an acceptable range. The isothermal process takes place from 0 to 3500 s, and after 3500 s is the heating phase. This shows that the SCR model can describe the ammonia adsorption and desorption process of the coated honeycomb SCR catalyst.

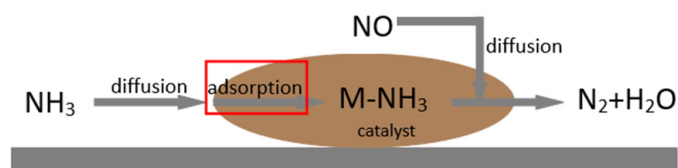


Figure 4. Schematic diagram of E-R mechanism.

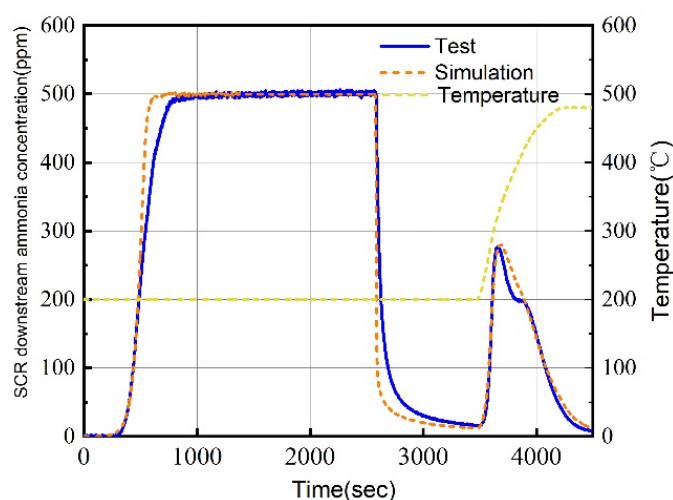


Figure 5. Comparison between NH₃ adsorption and desorption experiment and simulation results.

The essential evaluation indicators are the ammonia storage capacity of the catalyst, the ammonia oxidation efficiency, and the NO_x conversion efficiency. Figure 5 shows the verification results of the ammonia storage capacity of the SCR. Figure 6 compares the model ammonia oxidation efficiency and the experimental ammonia oxidation efficiency at different temperatures. As shown in Figure 6, the error between the ammonia oxidation efficiency predicted by the model and the ammonia oxidation efficiency measured by

the experiment is acceptable at different temperatures. This shows that the SCR model can reasonably predict the oxidation performance of ammonia under other temperature conditions. It can be seen from the figure that with the increase in temperature, the activity of the catalyst is more substantial; that is, the ammonia oxidation efficiency is higher.

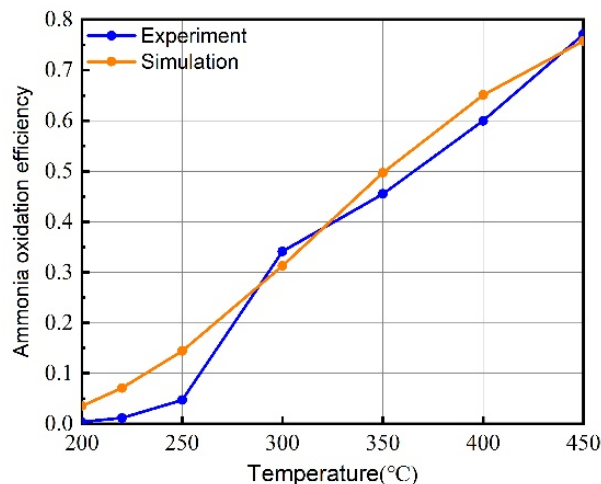


Figure 6. Comparison between experimental and simulation results of ammonia oxidation efficiency.

Figure 7a compares the standard SCR reaction NO_x conversion efficiency test results and simulation results. The figure shows that the experimental results are consistent with the temperature range of high NO_x conversion efficiency simulation results. Figure 7b compares the experimental results and the fast SCR reaction NO_x conversion efficiency simulation results. As shown in the figure, similarly, in the temperature range of high NO_x conversion efficiency, the experimental results are consistent with the simulation results. Figure 7c compares the experimental results and the slow SCR reaction NO_x conversion efficiency simulation results. As shown in the figure, although there is a difference between the experimental results and the simulation results in the low-efficiency temperature range, the error is within an acceptable range; moreover, in the high-efficiency NO_x conversion temperature range, the experimental results are consistent with the simulation results. Therefore, it shows that the SCR model can predict the NO_x conversion efficiency with different reaction speeds under other temperature conditions.

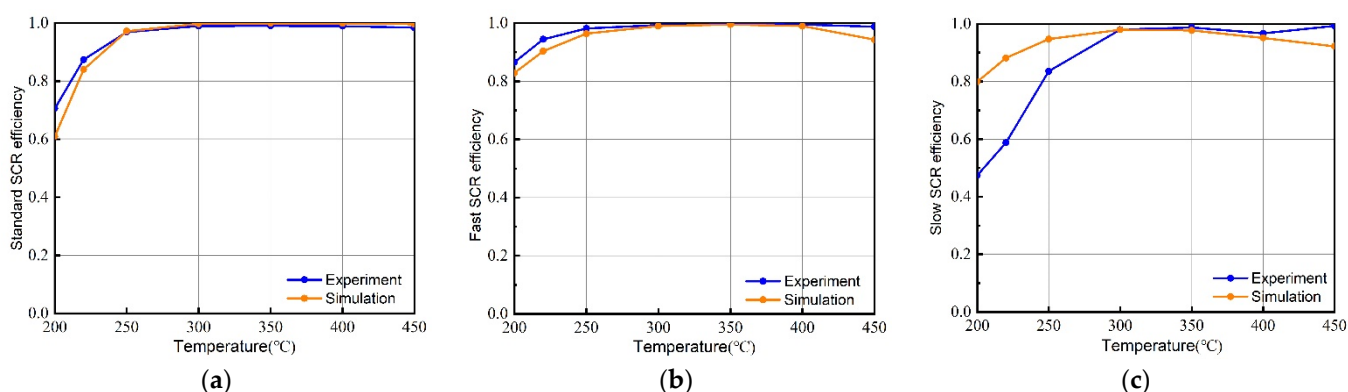


Figure 7. Comparison of NO_x conversion efficiency experiment and simulation results. (a) Comparison of standard SCR efficiency between experiment and simulation. (b) Comparison of fast SCR efficiency between experiment and simulation. (c) Comparison of slow SCR efficiency between experiment and simulation.

2.3. Research Method

The primary method of this study is to couple the one-dimensional SCR aftertreatment model with the three-dimensional CONVERGER engine model and analyze the NO_x conversion efficiency of the SCR aftertreatment model under different engine operating conditions. That is, the three-dimensional engine-related output emission parameters are used as the input parameters of the one-dimensional SCR model. This enables coupling between models across dimensions. At the end of the simulation of the verified three-dimensional CONVERGE engine model, the output data include the content distribution data of each emission in the cylinder of the engine model and the mass distribution of unburned ammonia and nitrogen oxides, but the mass distribution of emissions in the cylinder is not uniform. Firstly, to facilitate the analysis and calculation of relevant parameters, it is divided into grids with seemingly uniform emission quality in a small unit, such as the division method in Table 7 Step 1. Then, the unburned ammonia and nitrogen oxides in these grids are added to obtain the total unburned ammonia and nitrogen oxides in the cylinder with Step 2. In Step 3, the ratio *f* (mass fraction) obtained from the total mass of unburned ammonia and the total mass of nitrogen oxides can be used as the parameters of the one-dimensional SCR post-processing model. Similarly, other emissions can be used to input parameters into the one-dimensional SCR model.

Table 7. The main steps of transforming the output data of three-dimensional CONVERGE engine model into input parameters of the one-dimensional SCR aftertreatment model.

| Step 1: | | | Step 2: | Step 3: |
|---------|-----|----------|--|--|
| 1 | 2 | 3 | $\sum_{i=1}^n m_{\text{NH}_3}(i)$... $\sum_{i=1}^n m_{\text{total}}(i)$ | One-dimensional SCR model input parameters: $f = \frac{\sum_{i=1}^n m_{\text{NH}_3}(i)}{\sum_{i=1}^n m_{\text{total}}(i)}$ |
| 4 | 5 | 6 | | |
| ... | ... | ... | | |
| ... | ... | <i>n</i> | | |

Table 8 shows the main residual exhaust gas components and their proportions after in-cylinder combustion under three operating conditions for the ammonia–diesel dual-fuel engine, for which data were obtained using the above method. The three working conditions are random and different, but they have not reached the highest working condition of the engine, because the author needs to ensure that the exhaust temperature is within the temperature range of catalyst decomposition efficiency of nitrogen oxides, and there should be unburned ammonia in the excess state. It can be seen from Table 8 that the main residual waste in the cylinder of the ammonia–diesel dual-fuel engine is not only NO_x, but also a large amount of incompletely combusted ammonia, and the suitable temperature range of the catalyst is an important basis for the selection of these three working conditions. In addition, the proportion of unburned ammonia in the total emissions and the influence of a small amount of ammonia on NO_x reduction are also considered. Based on this, this study mainly investigates the reduction effect of the residual NH₃ in the cylinder on the residual NO_x when coupled with the SCR aftertreatment technology. This research aims to explore the effect of SCR on the emission reduction of unburned ammonia and nitrogen oxides of ammonia–diesel dual-fuel engines without additional urea, which is in the case without adding reducing gases such as ammonia into the model.

Table 8. Main residual exhaust gas and its concentration in the cylinder under different working conditions based on the 3D CFD simulation results.

| Example | NH ₃ (ppm) | NO (ppm) | NO ₂ (ppm) | N ₂ O (ppm) | Exhaust Temperature (°C) |
|---------|-----------------------|----------|-----------------------|------------------------|--------------------------|
| Case 1 | 1137.00 | 402.37 | 29.73 | 5.86 | 369 |
| Case 2 | 1202.12 | 462.01 | 34.59 | 11.03 | 371 |
| Case 3 | 720.70 | 437.37 | 59.53 | 16.64 | 369 |

3. Results and Analysis

3.1. NO_x Emission Reduction Efficiency Analysis

Firstly, the NO_x treatment results of the SCR model for Case 1 in Table 6 were analyzed. The NH_3 concentration input to the model was 1137.00 ppm, and no additional urea was added to the model. Figure 8a shows the NO emission reduction results of the SCR model. As shown in the figure, under the action of the catalyst, when a specific concentration of NO is introduced into the model, NO will be rapidly reduced to N_2 , and in this process, the emission of NO_2 is reduced; because the remaining NH_3 in the cylinder is in excess, the time for NO reduction is short, and the NO concentration at the SCR outlet is close to 0 after just 100 s. Figure 8b shows this model's NO_2 emission reduction results. As shown in the figure, since the emission of NO_2 in the cylinder is relatively low and the amount of NH_3 introduced is excessive, NO_2 can be quickly reduced. From the comparison of N_2O concentration at the inlet and outlet of the model in Figure 8c, it can be seen that the concentration at the N_2O outlet is increased by 50.64% relative to the inlet. However, since the emission of N_2O in the cylinder is relatively small, the amount of N_2O at the outlet of the model is also relatively small. However, even after the catalytic treatment of the SCR aftertreatment model, the emission of non-ammonia is still not optimistic, and the emission of N_2O only increases and does not decrease. From the comparison of NH_3 concentrations at the inlet and outlet of the SCR model in Figure 8d, it can be seen that the amount of NH_3 used to reduce NO is about half of the initial NH_3 amount. Therefore, the amount of ammonia introduced is in an excess state, and some ammonia is also adsorbed on the inner surface of the SCR; with this, the residual waste after the ammonia–diesel dual fuel is directly burned in the cylinder is passed into the SCR after-treatment device. Not only does it not need to add additional urea to the device, but it also reduces NO and unburned NH_3 emissions.

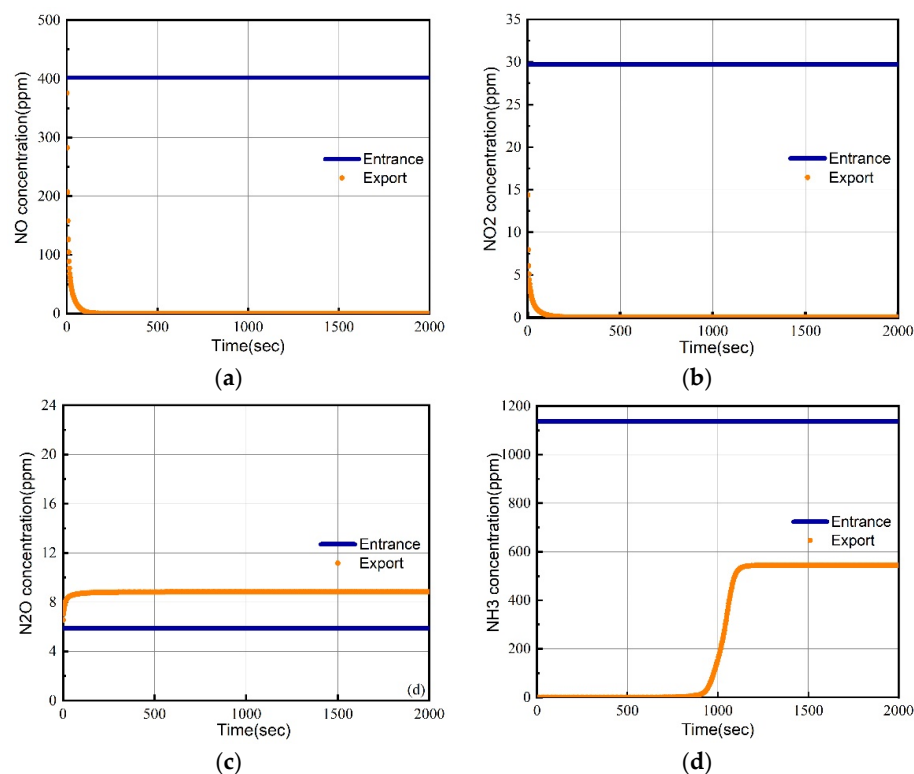


Figure 8. Comparison of NO_x and unburned ammonia concentrations at SCR inlet and outlet in Case 1. (a) NO concentration on entrance and export. (b) NO_2 concentration on entrance and export. (c) N_2O concentration on entrance and export. (d) NH_3 concentration on entrance and export.

Figure 9a shows the result of NO treatment of Case 2 by the SCR model. Compared with Figure 8a, it can be found that because there is a small difference in NO content between the inlets in Case 1 and Case 2, the treatment results are roughly the same; NO with a certain concentration is rapidly reduced to N_2 , thus reducing NO emission. Then, combined with the NO_2 emission reduction results of the SCR model in Figure 9b, it can be seen that under suitable temperature conditions, NO_2 can also be efficiently and rapidly reduced to N_2 , thereby reducing emissions. Combined with the processing results of Case 1 and Case 2 by the SCR model, it can be seen that the proportion of incompletely combusted ammonia in the combustion process of the ammonia–diesel dual-fuel engine is relatively large. The exhaust gas of the engine is directly passed into the aftertreatment without additional urea or NH_3 ; under suitable exhaust temperature, NO_x is efficiently and quickly reduced to N_2 , and the corresponding emission of NH_3 can also be reduced. Therefore, for ammonia and its dual-fuel engine exhaust emissions, the application of SCR aftertreatment technology can efficiently and quickly minimize NO_x emissions and reduce unburned ammonia emissions, playing a dual role in reducing emissions. Figure 9d shows the comparison of the treatment results of NH_3 in Case 2 by the SCR model. As shown in the figure, the concentration of ammonia at the outlet of the SCR is reduced by nearly 56.74% relative to the inlet, which significantly reduces the emission of unburned ammonia.

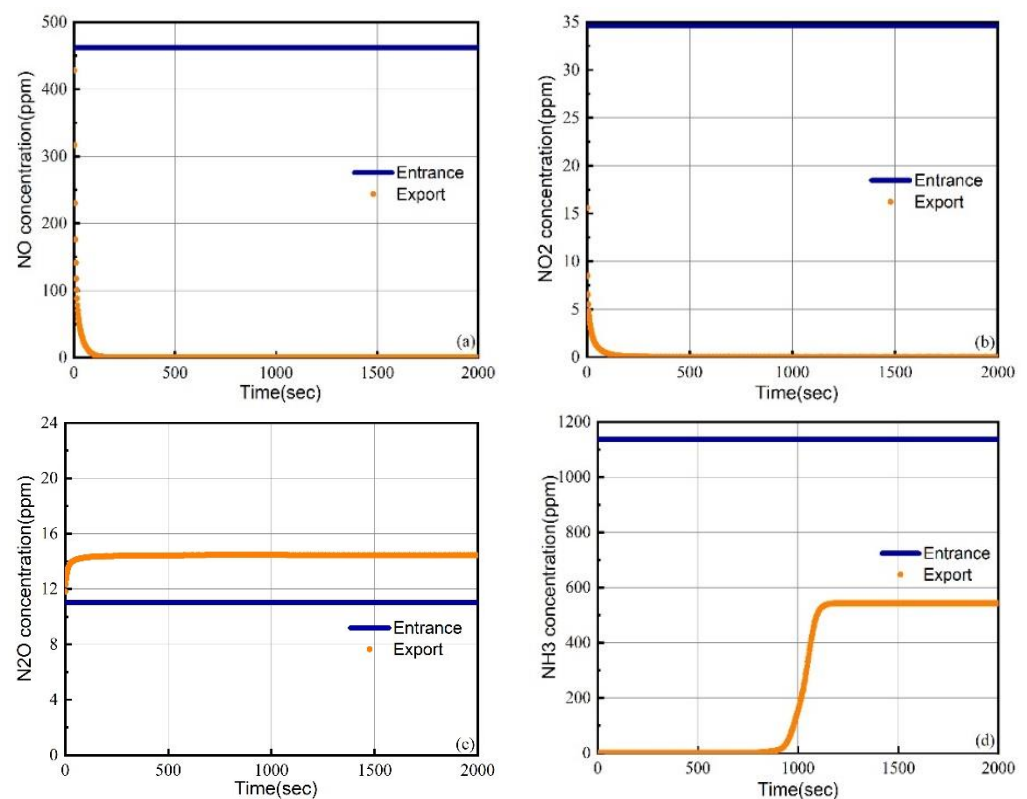


Figure 9. Comparison of NO_x and unburned ammonia concentrations at the SCR inlet and outlet in Case 2. (a) NO concentration on entrance and export. (b) NO_2 concentration on entrance and export. (c) N_2O concentration on entrance and export. (d) NH_3 concentration on entrance and export.

To further analyze the effect of a smaller amount of NH_3 on NO_x reduction compared to Case 1 and Case 2, the NO_x treatment results of the SCR model for Case 3 in Table 6 were analyzed; the unburned ammonia concentration was lower under this condition. Figure 10a compares NH_3 concentration at the inlet and outlet of the SCR model in case 3. As shown in the figure, the NH_3 concentration at the outlet of the model is almost 0, indicating that all the NH_3 introduced into the SCR model was adsorbed by the SCR and put into the reduction of NO_x . Figure 10b shows the comparison of NO concentration at the inlet and

outlet of the SCR model. As shown in the figure, in the case of an appropriate amount of ammonia, SCR can still efficiently reduce NO to N_2 . Nevertheless, NO reduction is slower compared with the excessive amount of ammonia. As shown in Figure 10c SCR model for NO_2 , the theoretical results show that, similarly, NO_2 can also be efficiently reduced to N_2 , and the time required is correspondingly about five times as long. Figure 10d shows the change in N_2O at the entrance and exit of the SCR model. As shown in Figure 10, the concentration of N_2O at the model's export has increased.

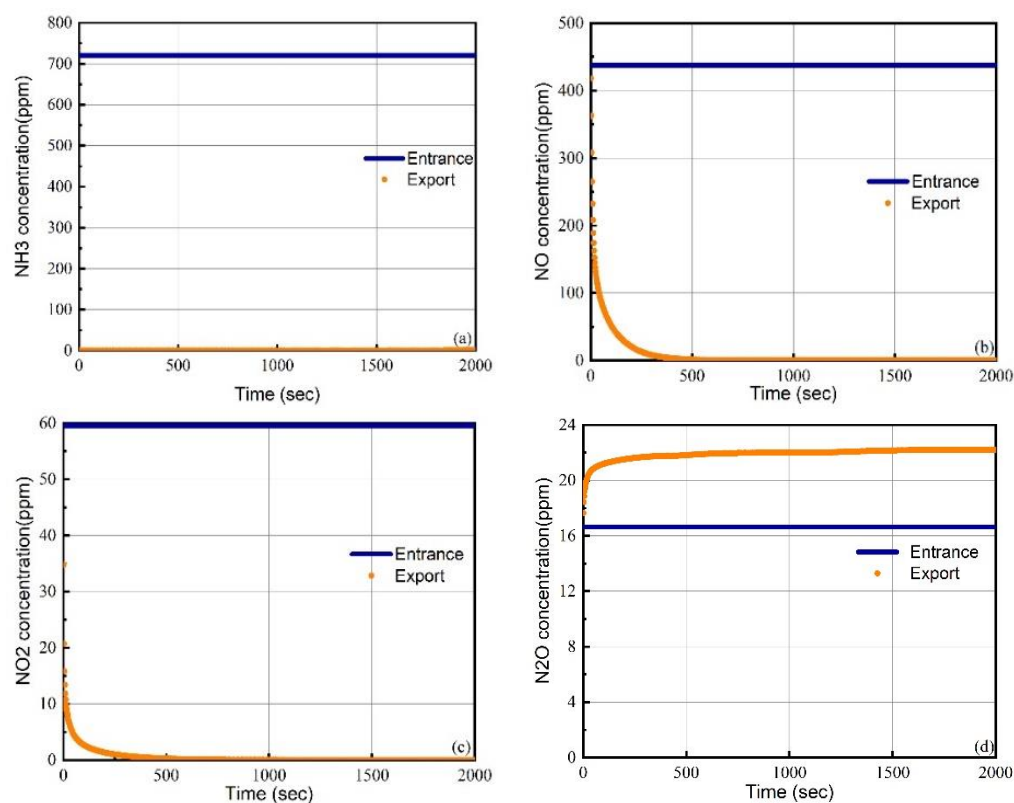


Figure 10. Comparison of NO_x and unburned ammonia concentrations at SCR inlet and outlet in Case 3. (a) NH_3 concentration on entrance and export. (b) NO concentration on entrance and export. (c) NO_2 concentration on entrance and export. (d) N_2O concentration on entrance and export.

Based on the above analysis, it can be seen that when the ammonia–diesel dual-fuel engine is combusted, the residual ammonia in the cylinder can be directly introduced into the SCR aftertreatment device as a reducing gas; thus, under the action of the catalyst, the exhaust NO_x under the same engine operating conditions can be reduced. It is efficiently reduced to N_2 and thus reduces its emissions. However, when the concentration of unburned ammonia in the exhaust gas of the ammonia–diesel dual-fuel engine is relatively large, an additional ammonia oxidation catalyst system will be required. In addition, it can be seen that N_2O concentration of ammonia–diesel engine exhaust gas will not decrease after SCR treatment, but also increase. The main reason is that NO_2 will be partially converted into N_2O under the action of the SCR catalyst, resulting in an increase in the concentration at the outlet. With the popularization and widespread use of ammonia-fueled engines, massive N_2O emissions will become an urgent problem to be solved under the circumstance that conventional SCR aftertreatment technology cannot reduce N_2O emissions. Furthermore, although the content of N_2O in the atmosphere is very low, its single-molecule warming potential is 298 times that of CO_2 ; that is, the greenhouse effect it can cause is 298 times that of CO_2 . It is listed as the third largest greenhouse gas after CO_2 and CH_4 . In second place, methane is 23 to 25 times more potent as a greenhouse gas than CO_2 . Therefore, the next section will analyze N_2O emission reduction measures.

3.2. Analysis of N₂O Generation, Decomposition Mechanism, and Emission Reduction Measures

3.2.1. N₂O Generation Mechanism and Decomposition Mechanism

Due to the different environmental conditions, such as the mixture composition and temperature in the combustion chamber at other times, the formation mechanism of N₂O is very complicated. The formation stages of N₂O are simplified into three steps: early combustion, middle combustion and late combustion. The research content of Yu et al. [48] includes the chemical reaction formula of N₂O formation from the mixture in the cylinder at these three stages. It is worth mentioning that the engine studied by Yu et al. is powered by gasoline, and for the combustion of ammonia and its blends, it can be concluded that the generation of N₂O mainly depends on the reaction $\text{NH}_2 + \text{NO}_2 = \text{N}_2\text{O} + \text{H}_2\text{O}$; therefore, this chemical reaction pathway needs to be analyzed in combination with relevant studies by Yu et al. In a three-way catalytic converter (TWC), molecules such as NO and CO are adsorbed on the catalyst surface, and NO is partially reduced to N₂O. This is similar to the principle that conventional SCR cannot reduce N₂O. Therefore, neither TWC nor conventional SCR can reduce N₂O emissions.

For N₂O in-cylinder decomposition, in the case of traditional hydrocarbon fuel combustion, its decomposition is mainly in the middle and late stages of combustion. At this time, the in-cylinder combustion temperature exceeds 2000 °C. Due to the short combustion duration, the incomplete combustion of CO, OH and other reducing molecules will reduce N₂O to N₂. In the reaction involving NH₃, the in-cylinder decomposition of N₂O mainly reduces it to N₂ with the help of reduction by the free hydrogen atom. Combined with the above analysis, the in-cylinder decomposition of N₂O has stringent requirements on temperature and concentration of reactants, so it is necessary to reduce N₂O emissions using out-of-cylinder aftertreatment technology.

3.2.2. Analysis of N₂O Emission Reduction by SCR after Treatment Technology

The studies of Daniells et al. [49] and Borsari et al. [50] showed that the catalyst of TWC can promote the reduction of N₂O to N₂ by CO when the temperature exceeds 400 °C. The studies of Liu et al. [51] showed that oxidation catalytic can reduce N₂O emissions from gasoline engine exhausts and that secondary gas supplementation technology can further reduce N₂O emissions from gasoline engine exhausts. Therefore, TWC can reduce N₂O emissions at high temperatures, but TWC generates N₂O when treating NO; Oxidation catalytic can reduce N₂O emissions, but cannot treat NO_x; oxidation catalytic couple with secondary gas supplementation technology can further reduce N₂O. Therefore, it is reasonable to speculate that oxygen supplementation technology is beneficial in reducing N₂O without oxidation catalytic.

Combined with the above research and analysis, it can be seen that feeding air or oxygen into the aftertreatment device can reduce the emission of N₂O; therefore, this study explores the effect of providing oxygen into the above SCR model on transform effects of N₂O, NH₃, and NO_x. As shown in Figure 11, before and after the introduction of oxygen into the model, the change in NO concentration had no significant impact; in contrast, the evolution of NO₂ concentration was substantial, mainly because after the introduction of oxygen, at low temperature (362 °C) and the action of the catalyst, NO reacts with oxygen first to generate NO₂, leading to a sharp increase in the concentration of NO₂. The concentration of ammonia at the outlet of the device is close to zero after the entire reaction is completed; and the introduction of oxygen into the model resulted in a decrease in the N₂O concentration at the outlet of the model, but the difference was not significant.

Therefore, the use of SCR technology can reduce NO_x and NH₃ emissions, but will increase N₂O emissions. Secondary oxygen supplementation technology can further reduce excess NH₃ and inhibit N₂O production within SCR to some extent, but will not reduce N₂O production obviously. For example, the basic N₂O at the inlet of SCR is 100 ppm, and the secondary oxygen supplementation technology is used, the N₂O at the outlet of SCR is slightly lower than 100 ppm. However, if the secondary oxygen supplementation technology is not adopted, when the basic N₂O at the inlet of SCR is 100 ppm, the N₂O at the outlet

of SCR may reach 150 ppm. Secondary oxygen supplementation technology needs to be combined with oxidation catalytic to reduce N_2O . Therefore, the recommended ammonia–diesel dual fuel engine aftertreatment configuration is SCR + oxygen supplementation + oxidation catalytic.

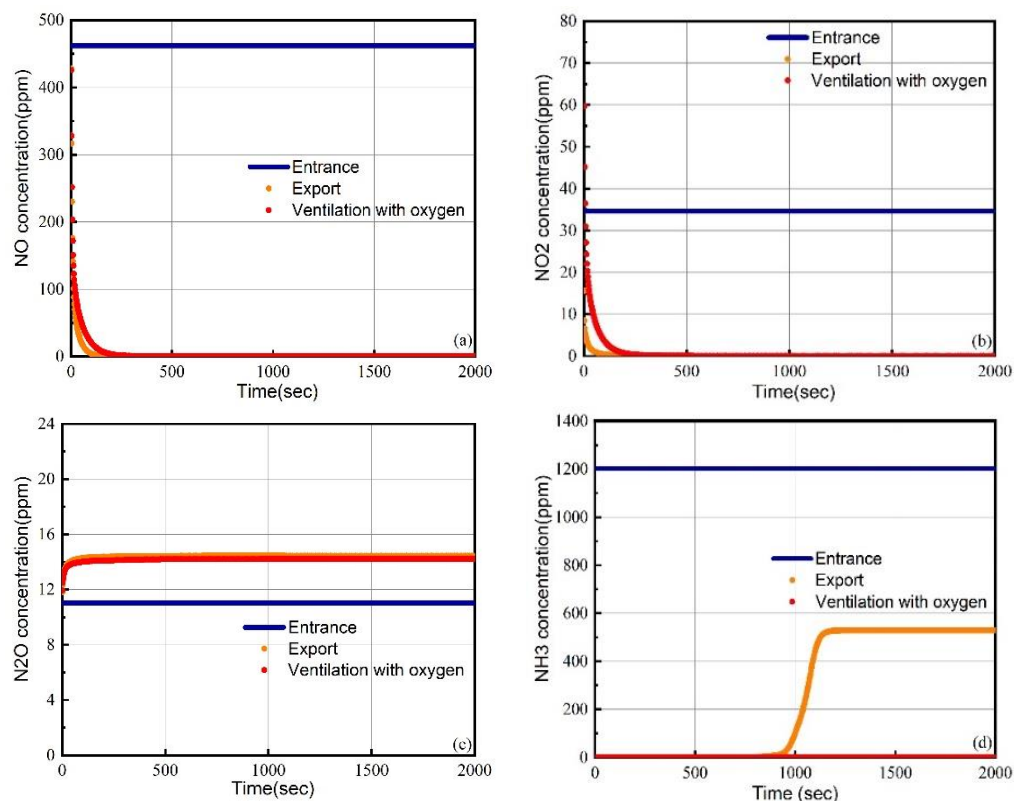


Figure 11. Changes in NO_x and ammonia concentrations at the inlet and outlet of the SCR model before and after oxygen was introduced in Case 2. (a) NO concentration on entrance, export and ventilation with oxygen. (b) NO_2 concentration on entrance, export and ventilation with oxygen. (c) N_2O concentration on entrance, export and ventilation with oxygen. (d) NH_3 concentration on entrance, export and ventilation with oxygen.

4. Conclusions

The ammonia–diesel dual-fuel engine inevitably emits large amounts of unburned ammonia and nitrogen oxides, which must be dealt with by the post-processor. So, in this study, the SCR aftertreatment model was first coupled with the 3D CONVERGE ammonia–diesel dual-fuel engine model in a one-dimensional form; according to parameters such as engine size, the aftertreatment model was modified to match the engine operating conditions; the test data verified the engine model and the SCR aftertreatment model, and verified the feasibility of the model. Then, according to the verified model, without additionally feeding reducing gases such as ammonia into the SCR model, the incompletely combusted ammonia in the diesel dual-fuel engine was fed into the SCR model to simulate the conversion efficiency of NO_x under the corresponding working conditions. Finally, because the conventional SCR model could not reduce the N_2O emission, the SCR model was treated with oxygen and its effect on reducing N_2O emissions was analyzed. The main conclusions are as follows:

- (1) A 3D ammonia–diesel dual-fuel engine model and 1D SCR aftertreatment model is developed and validated, the maximum burst pressure error is only 2.7%, and the two models are coupled across dimensions for the study of ammonia and NO_x removal effects. The effect that could not be presented by a single-dimensional simulation was obtained. The current study is based on the model, and the final actual

test verification of the engine aftertreatment joint platform has not been conducted. Subsequent relevant experiments will be further conducted to explore topics such as the influence of different combustion strategies and fuel injection strategies under working conditions on the nitrogen oxides and unburned ammonia in engine raw and pipe emissions.

- (2) On the premise that there is no need to inject ammonia and other reducing agents into the SCR, when the exhaust gas in the cylinder of an ammonia–diesel dual-fuel engine is isothermally passed into the model, NO and NO₂ can be 100% efficiently reduced to N₂ regardless of whether the ammonia concentration in the exhaust gas is excessive or equal NO_x is present in engine exhaust pipes, thereby reducing the NO_x emissions of the ammonia–diesel dual-fuel engine. However, when the concentration of unburned ammonia in the exhaust gas of the ammonia–diesel dual-fuel engine is large, the ammonia emission is still very high even after SCR aftertreatment. After SCR treatment, the concentration of N₂O in the exhaust gas of the ammonia–diesel dual-fuel engine has not decreased, but increases by about 50%. The main reason is that NO₂ will be partially converted into N₂O under the action of the SCR catalyst, resulting in an increase in the concentration at the outlet.
- (3) To achieve simultaneous removal of unburned ammonia, NO_x and N₂O, SCR + secondary oxygen supplementation and an oxidation catalyst are required. SCR mainly carries out the removal of NO, NO₂ and part of NH₃, secondary oxygen supplementation mainly removes excess ammonia, and an oxidation catalyst is used for N₂O removal. Injecting excess air or oxygen into the SCR aftertreatment model can not only significantly reduce the ammonia concentration at the outlet of the model without affecting the conversion efficiency of SCR to NO_x, but also inhibit the formation of N₂O within SCR, reducing the emissions of unburned ammonia and NO_x in the exhaust of ammonia–diesel dual-fuel engines. This ammonia (fuel)–SCR (without urea) system is one of the internal combustion engine technology routes to achieve zero carbon and nitrogen oxide emissions. Therefore, policy makers should support the vigorous development of internal combustion engines along this route, and explore the technical route for the engine to achieve high-ammonia fuel occupancy under all working conditions without additional urea injection.

Author Contributions: Conceptualization, X.S. and M.L.; methodology, H.L. and W.L.; validation, H.L., J.L. (Jincheng Li) and W.L.; formal analysis, M.L.; investigation, J.L. (Jincheng Li) and M.L.; resources, W.L.; data curation, C.W., X.D. and J.L. (Jingping Liu); writing—original draft preparation, M.L. and J.L. (Jincheng Li); writing—review and editing, M.L.; visualization, M.L.; supervision, H.L.; project administration, H.L.; funding acquisition, H.L. All authors have read and agreed to the published version of the manuscript.

Funding: This research was supported by the National Natural Science Foundation of China (Grant No. 52130605) and the Natural Science Foundation for Outstanding Young Scholars of Tianjin (Grant No. 20JCJQJC00160).

Data Availability Statement: The study did not report any data.

Acknowledgments: This research was supported by the National Natural Science Foundation of China (Grant No. 52130605) and the Natural Science Foundation for Outstanding Young Scholars of Tianjin (Grant No. 20JCJQJC00160).

Conflicts of Interest: The authors declare no conflict of interest.

References

1. Kappelle, M. *WMO Statement on the State of the Global Climate in 2019*; World Meteorological Organization (WMO): Geneva, Switzerland, 2020.
2. Montzka, S.A.; Dlugokencky, E.J.; Butler, J.H. Non-CO₂ greenhouse gases and climate change. *Nature* **2011**, *476*, 43–50. [[CrossRef](#)]
3. Thomas, G.; Parks, G. Potential Roles of Ammonia in a Hydrogen Economy—A Study of Issues Related to the Use Ammonia for On-Board Vehicular Hydrogen Storage. 2006. Available online: https://www.hydrogen.energy.gov/pdfs/nh3_paper.pdf (accessed on 19 January 2015).

4. Hollinger, T.; Vandenbrook, D.; Schiltz, M. Hydrogen and Ammonia Fuelled Internal Combustion Engine. International Patent WO2088/150901A1, 11 December 2008.
5. Reiter, A.J.; Kong, S.C. Demonstration of compression-ignition engine combustion using ammonia in reducing greenhouse gas emissions. *Energy Fuels* **2008**, *22*, 2963–2971. [[CrossRef](#)]
6. Grannell, S.M.; Assanis, D.N.; Gillespie, D.E. Exhaust emissions from a stoichiometric, ammonia and gasoline dual fueled spark ignition engine. In Proceedings of the Internal Combustion Engine Division Spring Technical Conference, Milwaukee, WI, USA, 3–6 May 2009; Volume 43406, pp. 135–141.
7. Yapicioglu, A.; Dincer, I. Performance assessment of hydrogen and ammonia combustion with various fuels for power generators. *Int. J. Hydrogen Energy* **2018**, *43*, 21037–21048. [[CrossRef](#)]
8. Zamfirescu, C.; Dincer, I. Ammonia as a green fuel and hydrogen source for vehicular applications. *Fuel Process. Technol.* **2009**, *90*, 729–737. [[CrossRef](#)]
9. Mørch, C.; Bjerre, A.; Gøttrup, M.; Sorenson, S.; Schramm, J. Ammonia/hydrogen mixtures in an SI-engine: Engine performance and analysis of a proposed fuel system. *Fuel* **2011**, *90*, 854–864. [[CrossRef](#)]
10. Gill, S.S.; Chatha, G.S.; Tsolakis, A. Assessing the effects of partially decarbonising a diesel engine by co-fuelling with dissociated ammonia. *Int. J. Hydrogen Energy* **2012**, *37*, 6074–6083. [[CrossRef](#)]
11. Zamfirescu, C.; Dincer, I. Using ammonia as a sustainable fuel. *J. Power Sources* **2008**, *185*, 459–465. [[CrossRef](#)]
12. Lasocki, J.; Bednarski, M.; Sikora, M. Simulation of ammonia combustion in dual-fuel compression-ignition engine. In Proceedings of the IOP Conference Series: Earth and Environmental Science, Moscow, Russia, 27 May–6 June 2019; IOP Publishing: Bristol, UK, 2019; Volume 214, p. 012081.
13. Dimitriou, P.; Javaid, R. A Review of ammonia as a compression ignition engine fuel. *Int. J. Hydrogen Energy* **2020**, *45*, 7098–7118. [[CrossRef](#)]
14. Ryu, K.; Zacharakis, G.; Kong, C. Effects of gaseous ammonia direct injection on performance characteristics of a spark-ignition engine. *Appl. Energy* **2014**, *116*, 206–215. [[CrossRef](#)]
15. Frattini, D.; Cinti, G.; Bidini, G. A system approach in energy evaluation of different renewable energies sources integration in ammonia production plants. *Renew. Energy* **2016**, *99*, 472–482. [[CrossRef](#)]
16. Armijo, J.; Philibert, C. Flexible production of green hydrogen and ammonia from variable solar and wind energy: Case study of Chile and Argentina. *Int. J. Hydrogen Energy* **2020**, *45*, 1541–1558. [[CrossRef](#)]
17. Zacharakis-Jutz, G.E. Performance Characteristics of Ammonia Engines Using Direct Injection Strategies. Ph.D. Thesis, Iowa State University, Ames, IA, USA, 2013.
18. Lhuillier, C.; Brequigny, P.; Contino, F. Experimental study on ammonia/hydrogen/air combustion in spark ignition engine conditions. *Fuel* **2020**, *269*, 117448. [[CrossRef](#)]
19. Valera-Medina, A.; Gutesa, M.; Xiao, H. Premixed ammonia/hydrogen swirl combustion under rich fuel conditions for gas turbines operation. *Int. J. Hydrogen Energy* **2019**, *44*, 8615–8626. [[CrossRef](#)]
20. Comotti, M.; Frigo, S. Hydrogen generation system for ammonia hydrogen fuelled internal combustion engines. *Int. J. Hydrogen Energy* **2015**, *40*, e10686. [[CrossRef](#)]
21. Frigo, S.; Gentili, R. Analysis of the behavior of a 4-stroke SI engine fuelled with ammonia and hydrogen. *Int. J. Hydrogen Energy* **2013**, *38*, 1607–1615. [[CrossRef](#)]
22. Wang, D.; Ji, C.; Wang, S. Numerical study of the premixed ammonia-hydrogen combustion under engine-relevant conditions. *Int. J. Hydrogen Energy* **2021**, *46*, 2667–2683. [[CrossRef](#)]
23. Li, J.; Huang, H.; Deng, L. Effect of hydrogen addition on combustion and heat release characteristics of ammonia flame. *Energy* **2019**, *175*, 604–617. [[CrossRef](#)]
24. Frigo, S.; Gentili, R.; Doveri, N. *Ammonia Plus Hydrogen as Fuel in a SI Engine: Experimental Results*; SAE Technical Paper; SAE: Warrendale, PA, USA, 2012.
25. Grannell, S.M.; Assanis, D.N.; Bohac, S.V. The fuel mix limits and efficiency of a stoichiometric, ammonia, and gasoline dual fueled spark ignition engine. *J. Eng. Gas Turbines Power* **2008**, *130*, 042802. [[CrossRef](#)]
26. Haputhanthri, S.O.; Maxwell, T.T.; Fleming, J. Ammonia and gasoline fuel blends for spark ignited internal combustion engines. *J. Energy Resour. Technol.* **2015**, *137*, 062201. [[CrossRef](#)]
27. Reiter, A.J.; Kong, S.C. Combustion and emissions characteristics of compression-ignition engine using dual ammonia-diesel fuel. *Fuel* **2011**, *90*, 87–97. [[CrossRef](#)]
28. Şahin, Z.; Akcanca, İ.Z.; Durgun, O. Experimental investigation of the effects of ammonia solution (NH₃OH) on engine performance and exhaust emissions of a small diesel engine. *Fuel* **2018**, *214*, 330–341. [[CrossRef](#)]
29. Ryu, K.; Zacharakis-Jutz, G.E.; Kong, S.C. Performance characteristics of compression-ignition engine using high concentration of ammonia mixed with dimethyl ether. *Appl. Energy* **2014**, *113*, 488–499. [[CrossRef](#)]
30. Gross, C.W.; Kong, S.C. Performance characteristics of a compression-ignition engine using direct-injection ammonia–DME mixtures. *Fuel* **2013**, *103*, 1069–1079. [[CrossRef](#)]
31. Bari, S.; Marian, R. Evolution of risk of diesel engine emissions on health during last 4 decades and comparison with other engine cycles: An innovative survey. In Proceedings of the ASME International Mechanical Engineering Congress and Exposition. American Society of Mechanical Engineers, Houston, TX, USA, 13–19 November 2015; Volume 57557, p. V012T15A004.

32. Manisalidis, I.; Stavropoulou, E.; Stavropoulos, A. Environmental and health impacts of air pollution: A review. *Front. Public Health* **2020**, *8*, 14. [[CrossRef](#)]
33. Peel, J.L.; Haeuber, R.; Garcia, V. Impact of nitrogen and climate change interactions on ambient air pollution and human health. *Biogeochemistry* **2013**, *114*, 121–134. [[CrossRef](#)]
34. Liu, L.; Wu, Y.; Wang, Y. Numerical investigation on the combustion and emission characteristics of ammonia in a low-speed two-stroke marine engine. *Fuel* **2022**, *314*, 122727. [[CrossRef](#)]
35. Li, T.; Zhou, X.; Wang, N.; Wang, X.; Chen, R.; Li, S.; Yi, P. A comparison between low-and high-pressure injection dual-fuel modes of diesel-pilot-ignition ammonia combustion engines. *J. Energy Inst.* **2022**, *102*, 362–373. [[CrossRef](#)]
36. Zheng, M.; Reader, G.T.; Hawley, J.G. Diesel engine exhaust gas recirculation—a review on advanced and novel concepts. *Energy Convers. Manag.* **2004**, *45*, 883–900. [[CrossRef](#)]
37. Capetillo, A.; Ibarra, F. Multiphase injector modelling for automotive SCR systems: A full factorial design of experiment and optimization. *Comput. Math. Appl.* **2017**, *74*, 188–200. [[CrossRef](#)]
38. Westlye, R.; Ivarsson, A.; Schramm, J. Experimental investigation of nitrogen-based emissions from an ammonia fueled SI engine. *Fuel* **2013**, *111*, 239–247. [[CrossRef](#)]
39. Kuta, K.; Przybyła, G.; Kurzydym, D.; Żmudka, Z. Experimental and numerical investigation of dual-fuel CI ammonia engine emissions and after-treatment with V₂O₅/SiO₂-TiO₂ SCR. *Fuel* **2023**, *334*, 126523. [[CrossRef](#)]
40. Niki, Y.; Yoo, D.H.; Hirata, K.; Sekiguchi, H. Effects of ammonia gas mixed into intake air on combustion and emissions characteristics in diesel engine. In Proceedings of the Internal Combustion Engine Division Fall Technical Conference, Greenville, SC, USA, 9–12 October 2016; American Society of Mechanical Engineers: New York, NY, USA, 2016; Volume 50503, p. V001T03A004.
41. Meisami-Azad, M.; Mohammadpour, J.; Grigoriadis, K.M. LPV gain-scheduled control of SCR aftertreatment systems. *Int. J. Control* **2012**, *85*, 114–133. [[CrossRef](#)]
42. Zhu, Y.; Xia, C.; Shreka, M. Combustion and emission characteristics for a marine low-speed diesel engine with high-pressure SCR system. *Environ. Sci. Pollut. Res.* **2020**, *27*, 12851–12865. [[CrossRef](#)]
43. Blinov, A.S.; Malastowski, N.S.; Myagkov, L.L. Numerical simulation of NO_x reduction in a SCR system. In Proceedings of the IOP Conference Series: Materials Science and Engineering, High Tatras, Slovakia, 13–15 October 2021; IOP Publishing: Bristol, UK, 2021; Volume 1111, p. 012009.
44. Niki, Y.; Nitta, Y.; Sekiguchi, H. Diesel fuel multiple injection effects on emission characteristics of diesel engine mixed ammonia gas into intake air. *J. Eng. Gas Turbines Power* **2019**, *141*, 061020. [[CrossRef](#)]
45. Luo, W.F. *Simulation Study on the Nitrogen Oxides Formation and Reduction Process of the Ammonia-Diesel Dual Fuel Engine*; Tianjin University: Tianjin, China, 2021.
46. Li, J.C.; Zheng, Z.Q.; Yao, M.F. Post-processing model. Matched two-stage SCR catalytic converters for heavy duty diesel engines Numerical simulation study. In Proceedings of the Chinese Society of Engineering Thermophysics Combustion Academic Annual Conference, Xiamen, China, 12–15 November 2020.
47. Nova, I.; Tonconi, E. *Urea-SCR Technology for deNO_x after Treatment of Diesel Exhausts*; Springer: New York, NY, USA, 2014.
48. Yu, X.X.; Sun, P.T.; Xia, Z.F. Formation mechanism and Emission control of N₂O. In Proceedings of the 2002 Annual Conference of Marine Mecha-Electronic and Communication Navigation Committee of China Institute of Navigation, Honolulu, HI, USA, 13–17 January 2002; pp. 37–39.
49. Burch, R.; Daniells, S.T.; Breen, J.P. A combined transient and computational study of the dissociation of N₂O on platinum catalysts. *J. Catal.* **2004**, *224*, 252–260. [[CrossRef](#)]
50. Borsari, V.; Assunção, J.V. Nitrous oxide emissions from gasohol, ethanol and CNG light duty vehicles. *Clim. Chang.* **2012**, *111*, 519–531. [[CrossRef](#)]
51. Liu, W.; Liu, S.J.; Wang, J. Formation mechanism and influencing factors of N₂O in general small gasoline engine. *J. Chin. Agric. Mech.* **2015**, *36*, 203–206.

Disclaimer/Publisher’s Note: The statements, opinions and data contained in all publications are solely those of the individual author(s) and contributor(s) and not of MDPI and/or the editor(s). MDPI and/or the editor(s) disclaim responsibility for any injury to people or property resulting from any ideas, methods, instructions or products referred to in the content.